The quasi-electrostatic mode of chorus waves and electron nonlinear acceleration

O. V. Agapitov, A.V. Artemyev, D Mourenas, V Krasnoselskikh, J Bonnell, Olivier Le Contel, C. M. Cully, V Angelopoulos

AGU PUBLICATIONS

JGR

Journal of Geophysical Research: Space Physics

RESEARCH ARTICLE

10.1002/2013JA019223

The quasi-electrostatic mode of chorus waves and electron nonlinear acceleration

O. V. Agapitov[1,2,3], A. V. Artemyev[1,4], D. Mourenas[5], V. Krasnoselskikh[1], J. Bonnell[2], O. Le Contel[6], C. M. Cully[7], and V. Angelopoulos[8]

[1]LPC2E/CNRS, University of Orleans, Orleans, France, [2]Space Sciences Laboratory, University of California, Berkeley, California, USA, [3]Astronomy and Space Physics Department, National Taras Shevchenko University of Kiev, Kiev, Ukraine, [4]Space Research Institute, RAS, Moscow, Russia, [5]CEA, DAM, DIF, Arpajon, France, [6]LPP/CNRS, Ecole Polytechnique, Paris, France [7]Department of Physics and Astronomy, University of Calgary, Calgary, Alberta, Canada [8]Institute of Geophysics and Planetary Physics, Department of Earth and Space Sciences, University of California, Los Angeles, California, USA

Key Points:
- Chorus may propagate in a quasi-electrostatic mode
- The parallel component of wave electric field is about 25%
- The large parallel wave electric field can trap electrons into Landau resonance

Correspondence to:
O. V. Agapitov,
oleksiy.agapitov@gmail.com

Citation:
Agapitov, O. V., A. V. Artemyev, D. Mourenas, V. Krasnoselskikh, J. Bonnell, O. Le Contel, C. M. Cully, and V. Angelopoulos (2014), The quasi-electrostatic mode of chorus waves and electron nonlinear acceleration, *J. Geophys. Res. Space Physics*, *119*, 1606–1626, doi:10.1002/2013JA019223.

Received 17 JUL 2013
Accepted 6 FEB 2014
Accepted article online 10 FEB 2014
Published online 5 MAR 2014

Abstract Selected Time History of Events and Macroscale Interactions During Substorms observations at medium latitudes of highly oblique and high-amplitude chorus waves are presented and analyzed. The presence of such very intense waves is expected to have important consequences on electron energization in the magnetosphere. An analytical model is therefore developed to evaluate the efficiency of the trapping and acceleration of energetic electrons via Landau resonance with such nearly electrostatic chorus waves. Test-particle simulations are then performed to illustrate the conclusions derived from the analytical model, using parameter values consistent with observations. It is shown that the energy gain can be much larger than the initial particle energy for 10 keV electrons, and it is further demonstrated that this energy gain is weakly dependent on the density variation along field lines.

1. Introduction

The Earth's Van Allen radiation belts are known to constitute a very efficient accelerator of relativistic particles [*Millan and Baker*, 2012]. One of the key processes responsible for particle acceleration and particle scattering in the radiation belts is wave-particle interaction, especially with whistler mode waves. The frequency of these waves is a fraction of the electron gyrofrequency. The most intense whistler waves observed in the belts and in the outer terrestrial magnetosphere are discrete ELF/VLF (extremely low frequency/very low frequency) electromagnetic emissions known as chorus. They are important for the dynamics of the outer radiation belt as they play a crucial role in the local acceleration and losses of energetic electrons [*Shprits et al.*, 2008; *Ukhorskiy and Sitnov*, 2012]. These magnetospherically generated emissions are characterized by rising and falling tones with frequencies ranging from a few hundred hertz to several kilohertz (see reviews by *Sazhin and Hayakawa* [1992] and *Omura et al.* [1991]). Whistler waves propagate in a right-hand polarized mode and in a wide range of wave normal directions from quasi parallel to the background magnetic field (with circular polarization) to quasi transverse (then waves become quasi electrostatic with close to linear polarization) (see statistics in *Li et al.* [2011a] and *Agapitov et al.* [2013]).

The timescales of particle acceleration processes in the magnetosphere vary over a large range from seconds to days. A widely used approach for evaluating particle scattering and acceleration due to interaction with uncorrelated small-amplitude waves is the quasi-linear theory of diffusion of the particle velocity distribution function [*Romanov and Filippov*, 1961; *Drummond and Pines*, 1962; *Vedenov et al.*, 1962]. An application of this approach for the description of radiation belt dynamics was proposed by *Trakhtengerts* [1966] and *Kennel and Petschek* [1966]. The principal elements of such a description are pitch angle and energy diffusion coefficients (the latter being mainly responsible for energy transfer). The characteristic timescales for such an interaction depend on geomagnetic activity, but even for a very disturbed magnetosphere, they are not less than hours. The diffusion coefficients were calculated using a quasi-linear approximation [*Lyons et al.*, 1972; *Lyons*, 1974; *Glauert and Horne*, 2005; *Shprits et al.*, 2006; *Summers et al.*, 2007, and references therein] and are widely used in global radiation belt codes for the solution of the Fokker-Planck equation for velocity distributions [e.g., *Bourdarie et al.*, 1996; *Varotsou et al.*, 2008; *Fok et al.*, 2008; *Subbotin et al.*, 2010].

However, recent reports of large-amplitude whistlers [*Cattell et al.*, 2008; *Cully et al.*, 2008; *Li et al.*, 2011a; *Kellogg et al.*, 2011] have raised the question of whether the traditionally employed diffusion-based models are adequate for describing radiation belt dynamics. More efficient particle energy changes can occur due to interaction with coherent, large-amplitude waves. Large wave amplitudes give rise to nonlinear mechanisms of wave-particle interaction, including particle trapping (see review by *Shklyar and Matsumoto* [2009]). *Kellogg et al.* [2010] have provided experimental evidence that such trapping really occurs in the inner magnetosphere.

A number of studies of the source and propagation properties of chorus emissions indicate that chorus propagate initially along the background magnetic field in the equatorial source region [*Li et al.*, 2012; *Santolík et al.*, 2005]. Thus, most of the works until now have considered quasi-parallel whistler wave propagation at all geomagnetic latitudes. However, recent satellite observations show that wave normals can be highly oblique and already tend to the resonance cone at latitudes $\lambda \sim 20°$–$30°$ [*Agapitov et al.*, 2012, 2013], which is consistent with the results of numerical ray tracing studies [*Bortnik et al.*, 2011; *Breuillard et al.*, 2012; *Chen et al.*, 2013]. *Santolík et al.* [2009] and *Chum et al.* [2009] analyzed in details some nightside chorus events by using Cluster measurements and found that chorus can also be generated with highly oblique wave normals (several degrees from the resonance cone). A population of similarly very oblique waves has also been pointed out in Time History of Events and Macroscale Interactions During Substorms (THEMIS) statistics in the vicinity of the equator [*Li et al.*, 2011a, 2013]. The wave normal angle distribution is a critical parameter for considering wave-particle interaction in both the quasi-linear and nonlinear approaches. The statistical significance of oblique waves demonstrated in *Agapitov et al.* [2012, 2013] has an important impact on electron acceleration and scattering in the quasi-linear approach [*Artemyev et al.*, 2012a; *Mourenas et al.*, 2012b, 2012a] and in the nonlinear approach [*Shklyar and Matsumoto*, 2009; *Artemyev et al.*, 2012b] for extremely large-amplitude whistler waves. The wave normal distributions obtained by *Agapitov et al.* [2012, 2013] from Cluster statistics and the related increase of the wave electric field with latitude can lead to the presence of a large electric field component along the background magnetic field, especially when reminding that *Agapitov et al.* [2011b, 2013] only present amplitudes averaged over 4 s, which can be 1 order of magnitude smaller than actual wave amplitudes [*Cully et al.*, 2008]. The relatively common occurrence of coherent oblique whistler waves with large amplitudes [*Cattell et al.*, 2008; *Cully et al.*, 2008; *Wilson et al.*, 2011; *Kellogg et al.*, 2011; *Li et al.*, 2011a, 2011b, 2013] and their high efficiency in wave-particle interaction imply that such local acceleration and scattering processes have to be taken into account for accurately modeling the radiation belts dynamics.

In this paper, we present a multicase study of large-amplitude chorus waves propagating in a quasi-electrostatic mode with wave normal angles very close to the resonance cone, on the basis of six component measurements aboard the THEMIS spacecraft at a magnetic latitude $\lambda \leq 15°$. Next, analytical estimates of the corresponding acceleration of trapped electrons are derived and further compared with test-particle simulations, demonstrating the potential importance of such a process in radiation belt dynamics.

2. Data Description and Processing Technique

THEMIS (Time History of Events and Macroscale Interactions During Substorms) consists of five identically instrumented spacecraft (THA, THB, THC, THD, and THE), launched on 17 February 2007. The main goal of this mission is to conduct multipoint investigations of substorm phenomena in the tail of the terrestrial magnetosphere [*Sibeck and Angelopoulos*, 2008]. For the current study, search coil magnetometer (SCM) observations [*Le Contel et al.*, 2008] and plasma measurements of the electric field instrument [*Bonnell et al.*, 2008] were analyzed. The three search coil antennas cover the same bandwidth, from 0.1 Hz to 4 kHz, in the VLF/ELF range. The electric field components are measured directly in the same frequency range. Three components of magnetic field waveform and three components of electric field waveform captured in the wave burst mode (onboard trigger) with 8192 samples per second were used. The fluxgate magnetometer (FGM) [*Auster et al.*, 2008] provides measurements of three components of the background magnetic fields with a sampling of up to 64 Hz. In the current study, the FGM data are used to evaluate the local electron cyclotron frequencies and to define the background magnetic field, so that a 3 s sampling of the data is applied. We use the spin-averaged FGM data with 3 s time resolution and spline interpolation to determine magnetic fields in between them.

AGU Journal of Geophysical Research: Space Physics
10.1002/2013JA019223

Table 1. Parameters of Observed High-Amplitude Waves

N	SC	Date[a]	UT	Magnetic Latitude(deg)	L	Magnetic Local Time	$\theta(\theta_{res})$(deg)	f_{ce}(Hz)	f/f_{ce}(Hz)	$E_{\|\|}/\|E\|$	E_{min}/E_{max}	$\|\mathbf{E}_{max}\|$ (mV/m)
1	THE	2007-11-14	03:35:07	14.45	4.3	9.8	63(70.6)	12111	~0.3	0.3 (0.32)	0.25	150
2	THA	2008-12-5	22:17:32	−14.0	6.4	13.3	66(73.4)	4551	0.27	0.32(0.31)	0.55	70
3	THA	2008-12-5	22:17:32	−14.0	6.4	13.3	66(73.4)	4551	0.26–0.28	0.33(0.2)	0.6	70
4	THC	2007-8-7	18:41:49	11.7	5.2	11.1	68(70.1)	7082	0.33	0.05(0.1)	0.86	80
5	THC	2007-8-28	15:51:48	15	5.4	7.1	74(78.6)	1400	0.19	0.17(0.21)	0.31	40
6	THA	2008-11-26	03:18:23	0	5.0	12.0	57(60.3)	6051	~0.48	0.37(0.38)	0.23	200
7	THE	2008-11-17	00:38:54	−12.8	6.9	13.7	68(75.4)	3600	0.25	0.26(0.24)	0.27	55
8	THA	2008-12-7	03:32:47	−1.17	6.0	3.0	63(72.0)	3000	0.31	0.33(0.29)	0.19	30
9	THA	2008-11-27	22:38:46	−13.8	6.3	13.5	70(75.8)	4480	0.24	0.24(0.27)	0.24	65
10	THA	2008-11-26	21:48:05	−13.7	7.6	9.1	74(68.7)	1932	0.36	0.16(0.11)	0.78	100
11	THA	2008-11-25	22:29:04	−13.8	6.5	9.7	67 (72.9)	4090	0.29	0.26(0.29)	0.32	55
12	THA	2008-10-23	03:58:14	−18.7	6.5	12	76(76.3)	5078	0.23	0.32(0.25)	0.38	40
13	THC	2007-8-11	16:41:56	16.1	5.4	7.7	75(76.2)	8293	0.23	0.17(0.12)	0.41	100
14	THC	2007-9-6	18:24:30	6.5	4.6	6.1	44(65.8)	8300	0.4	0.33(0.26)	0.14	60
15	THC	2007-9-6	19:17:28	4.8	6.2	6.9	44(68.9)	8300	0.36	0.33(0.38)	0.16	40

[a]Dates are formatted as year-month-day.

In this study, a whole set of techniques for wave polarization estimation (such as the Means method [*Means*, 1972], minimum variance analysis of the spectral variation matrix, and singular value decomposition (SVD) [*Santolík et al.*, 2003]) is used to determine the wave normal angle, wave ellipticity (defined as the ratio of the minor axis to the major axis in the plane perpendicular to the wave normal), and planarity (i.e., the ratio of polarized power to total power, which actually determines the applicability of the single planar wave approximation). To reduce the uncertainties caused by enhanced noise level in the electric field measurements along spacecraft spin, we use only magnetic field measurements for the SVD method. In this case all these methods have an inherent 180° ambiguity in the wave normal direction, but this ambiguity can be removed if the Poynting vector $\vec{S}$ is known. Since the wave normal vector must have a component in the direction of the energy flow, the scalar product $(\vec{S} \cdot \vec{k})$ should be positive. The Poynting vector is calculated directly: $\vec{S} = (1/2)\mathrm{Re}(\vec{E}(f) \times \vec{B}(f)^*)$, where * represents the complex conjugate, R*e* stands for the real part, and $\vec{E}(f)$ and $\vec{B}(f)$ are the Fourier transforms of the electric and magnetic field waveforms, respectively.

3. Observations

The relatively frequent occurrence of high-amplitude coherent whistler waves demonstrated in the works by *Cattell et al.* [2008], *Wilson III et al.* [2011], and *Li et al.* [2011a, 2013] on the basis of STEREO, Wind, and THEMIS data has allowed us to collect a whole set of large-amplitude (>40 mV/m) whistler wave events detected by the THEMIS spacecraft in 2007–2008. The corresponding chorus wave events are listed in Table 1. The wave normal angles θ (with respect to the background magnetic field) were obtained from magnetic field waveform data (SCW) and are given in Table 1: all the observed chorus wave packets are very oblique, with values of θ close to the local resonance cone angle θ_{res} (listed in round brackets). These wave events were captured over a wide range of magnetic latitudes (λ varying from −20° to 20°; see in Table 1), but no dependence of θ on λ was observed (for λ dependence see the large statistics presented by *Li et al.* [2013]). Ray tracing reconstruction of wave propagation for the wave events detected at $\lambda \sim 15°$ shows that these waves were generated with quite oblique wave normal from 35° to 55° taking as initial condition an equatorial generation (see also similar results of backward ray tracing in *Lauben et al.* [2002]).

Wave amplitudes vary from 40 to 300 mV/m. Due to their obliqueness, there is a significant component of wave electric field along the background magnetic field. The parallel component to full wave electric field ratios are listed in Table 1 (the values of $E_{||}/|E|$ reconstructed by use of θ from SCM measurements are listed in round brackets). The magnitude of the parallel electric field depends on θ and varies from 0.05 to 0.4 of the full wave electric field perturbation, corresponding to 20–100 mV/m. The waveforms of the wave packets listed in Table 1 are shown in Figure 1, where the electric field component parallel to the background magnetic field is shown in red. For such oblique propagation, electric field polarization changes from circular to elliptical with E_{max}/E_{min} about 2–7, and close to linear in cases 8, 14, and 15. Polarization of the wave electric field is displayed in Figure 2 in the form of the hodographs of electric field in a plane determined by minimum variance analysis. It is necessary to note that wave frequency in cases 6,14, and 15 is close to the Nyquist frequency, which results in the observed form of the hodographs: 2–3 measurements during one wave period. The wave perturbations seen in the magnetic field are generally weak and their amplitudes may be close to the background noise level. Magnetic field polarization, even for a wave normal angle close to the resonance cone, is elliptical with B_{max}/B_{min} about 1.1–1.5, which allows determining the wave normal with some degree of confidence. The ratio of magnetic and electric field magnitudes confirms the estimated values of θ and the electric field polarization. Note that we restrict our consideration to the general analysis of waveforms without any detailed investigation of the inner structure of these forms. Although such an investigation can be useful for analyzing the effects of trapped electrons [see *Kellogg et al.*, 2010], we mainly focus here on wave properties which can be directly used in our further modeling of the wave-particle resonant interaction.

A summary of observed wave properties is provided in Figure 3. The dependence of the observed ratio $E_{||}/|E|$ on the wave frequency f to local electron gyrofrequency f_{ce} ratio is displayed. Electric field wave amplitude and polarization are indicated by size and form of symbols. We use the Minimum Variance Analysis (MVA) method to determine the ratio between the axes of the polarization ellipse of the electric field. The error bars are determined from the relations between the corresponding eigenvalues [see *Khrabrov and Sonnerup*, 1998]. The inferred $E_{||}/|E|$ values in the covered f/f_{ce} range are shown by dashed lines with colors related to θ values and listed in the figure legend. The values of $E_{||}/|E|$ corresponding to the resonance cone angle and to the Gendrin angle $\theta_g \sim \arccos(2f/f_{ce})$ are indicated by the black dotted line and red solid

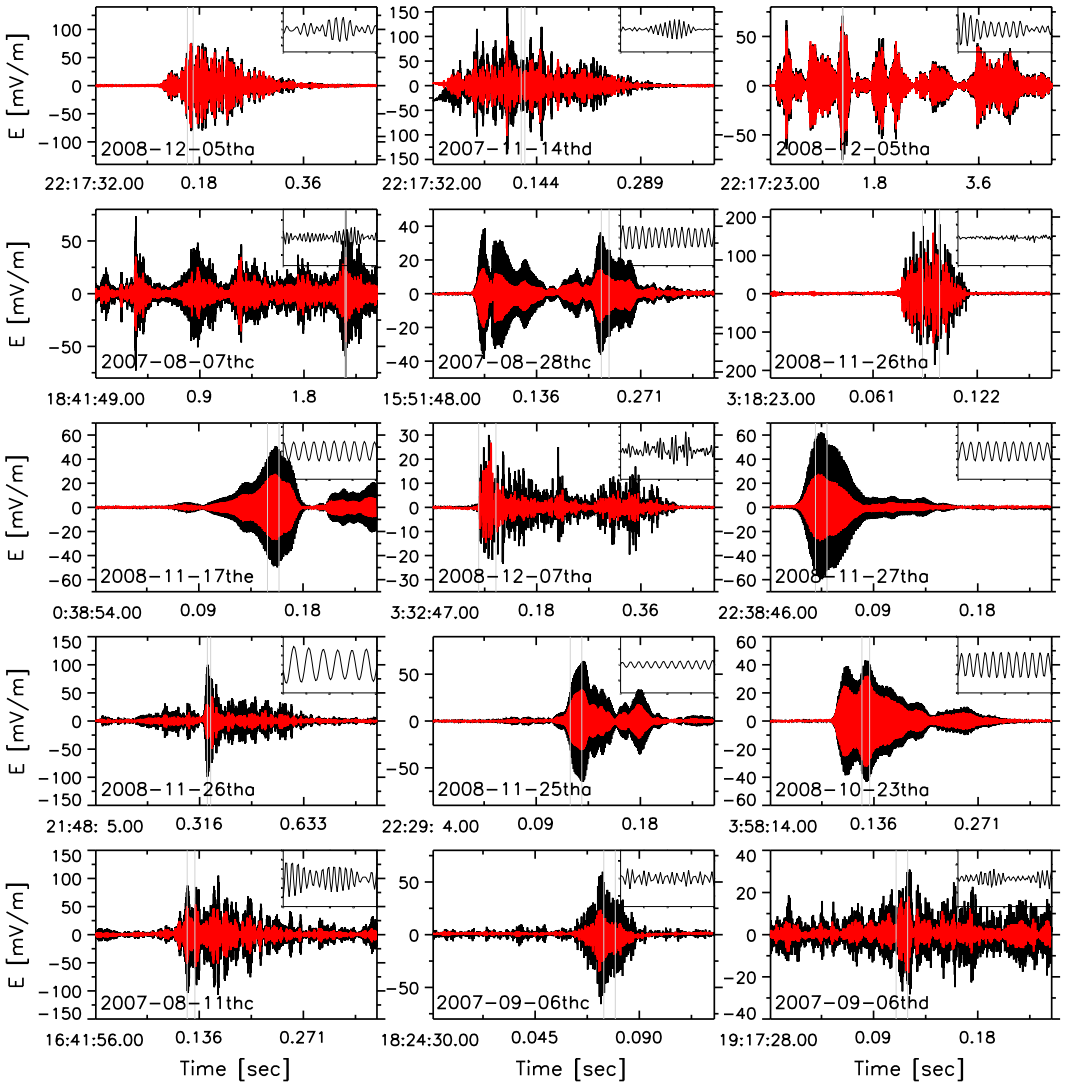

Figure 1. Wave electric field waveforms captured by THEMIS spacecraft. The component parallel to the background magnetic field is indicated in red. The details concerning these events are listed in Table 1. The small panels show the detailed waveform for the time range indicated by grey vertical lines in the similar amplitude scale as the corresponding large panel.

line, respectively. Here we use approximate expressions for Gendrin and resonance cone angles strictly valid only for a plasma frequency to gyrofrequency ratio larger than 2–3. THEMIS measurements correspond to the nearly equatorial region $|\lambda|<20°$ where such an approximation looks reasonable. Our analysis of the detected large-amplitude chorus waves shows that these waves are both coherent and oblique ($\theta \sim \theta_g$ or even $\theta > \theta_g$) and thus have a significant electric field component along the background magnetic field. During the propagation, θ can increase up to the resonance cone angle, while the wave amplitude can simultaneously increase until reaching a maximum around $\lambda \sim 5°–10°$ [*Agapitov et al.*, 2013] where Landau damping should enter into play [*Chen et al.*, 2013]. Accordingly, $E_{\parallel}$ should increase and attain its maximum value at $\lambda \sim 10°–15°$. There, assuming that the considered whistler waves become quasi-electrostatic with $\sin\theta \sim 1$, one obtains $E_{\parallel} \sim Ef/f_{ce}$ (see the relationships between wave components in *Ginzburg and Rukhadze* [1975])

4. Resonant Acceleration

In this section, we consider the effect of observed high-amplitude oblique whistler waves on resonant electron acceleration. Wave amplitudes substantially exceed the level required for nonlinear interaction

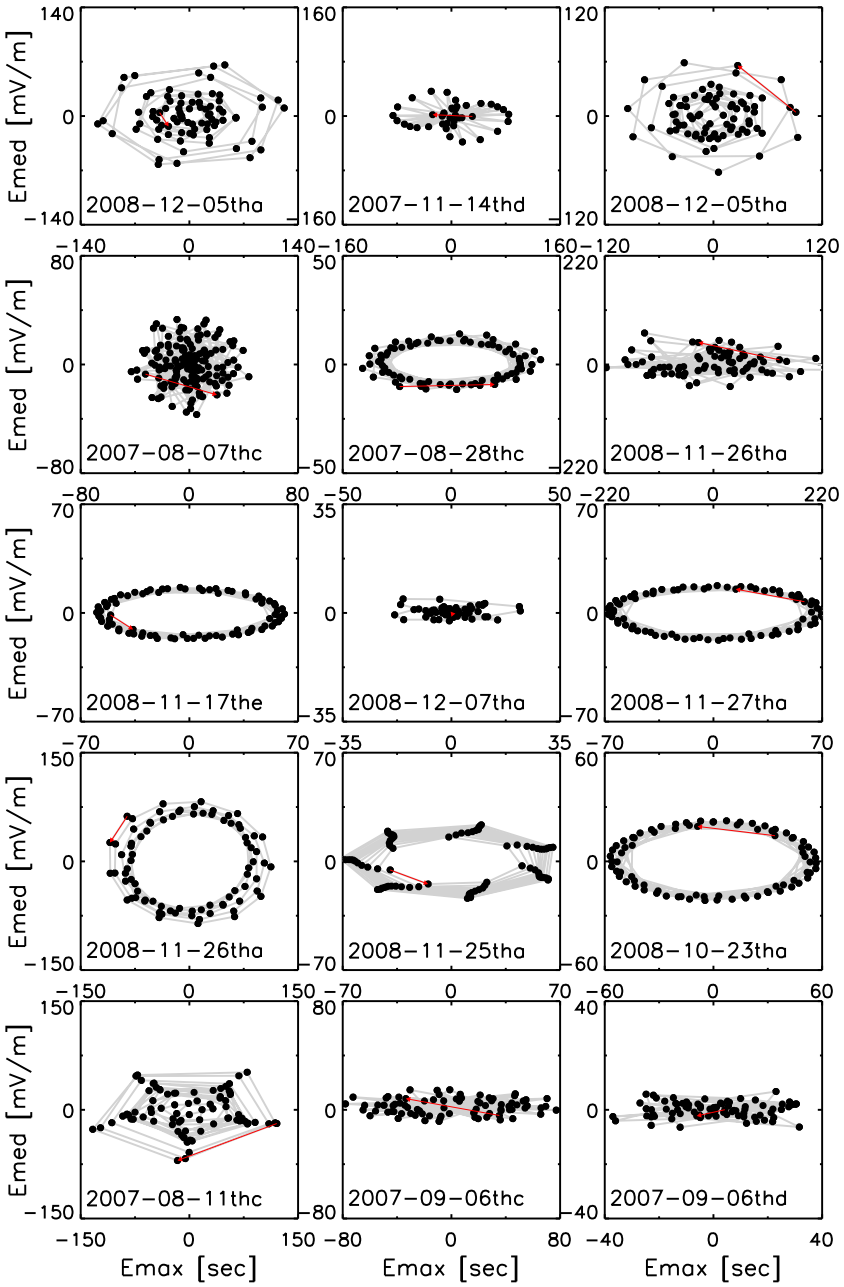

Figure 2. Hodographs of wave electric field in the plane determined by minimum variance analysis of electric field perturbations for events listed in Table 1.

(see discussion below, papers by *Bell* [1986] and *Shklyar and Matsumoto* [2009, and references therein]), so that electron trapping by these waves has to be considered. The general theory of wave-particle nonlinear interaction, including the process of trapping in an inhomogeneous magnetic field, originates from pioneering papers by *Dysthe* [1971], *Nunn* [1971], and *Karpman et al.* [1974, 1975]. This theory is based on an adiabatic description of charged particle motion in the wave potential [e.g., *Kolomenskii and Lebedev*, 1963; *Davydovskiĭ*, 1963; *Roberts and Buchsbaum*, 1964; *Laird and Knox*, 1965; *Bell*, 1965]. There are several important generalizations of this theory: stochastization of relativistic electron motion due to magnetic field inhomogeneity was considered by *Shklyar* [1981] and *Albert* [1993]; a comprehensive description of nonrelativistic electron resonant interaction with oblique whistler waves can be found in a review by [*Shklyar and Matsumoto* 2009]; and the effect on particle acceleration of a decrease of the electron gyrofrequency due to a large relativistic factor was described by *Omura et al.* [2007]. The effects on particle acceleration of a

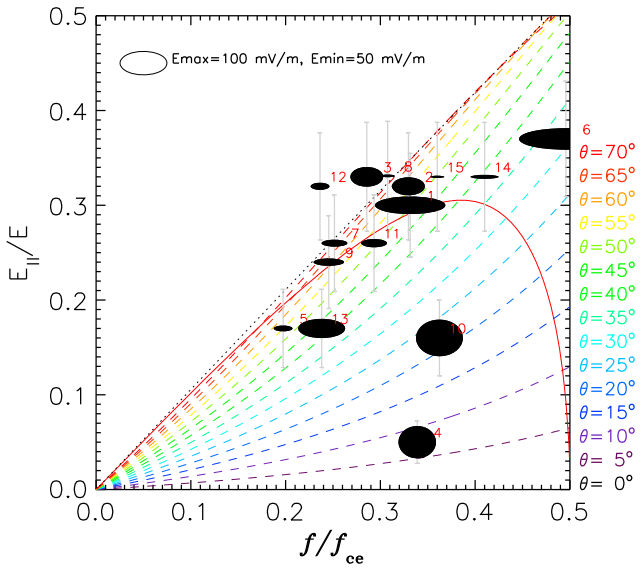

Figure 3. Dependence of observed ratio $E_{||}/|E|$ on f/f_{ce} for events listed in Table 1. Electric field wave amplitude and polarization are indicated by size and form of symbols. Calculated $E_{||}/|E|$ values for the considered f/f_{ce} range are shown by dashed lines with colors related to θ values and listed in legend. The resonance cone angle and the value of $E_{||}/|E|$ corresponding to the Gendrin angle $\theta_g \sim \arccos(2f/f_{ce})$ are indicated by black dotted and red solid lines, respectively.

variation of the wave normal angle and frequency of the wave in the course of propagation were first analyzed by *Bell* [1984, 1986]. This investigation was later generalized to relativistic electrons by *Katoh et al.* [2008] and for a particular dependence of the wave frequency on its amplitude by *Demekhov et al.* [2006]. Acceleration by a wave of nonuniform amplitude (the effect of modulation) was recently studied by *Tao et al.* [2012].

The resonance condition of electron interaction with whistler waves has a form

$$\omega - k_{||}v_{||} = -n\Omega_c/\gamma,$$

where $k_{||} = k\cos\theta$ (k denoting wave number), $v_{||}$ is the electron parallel velocity, and the wave frequency ω is typically several times smaller than the electron cyclotron frequency Ω_c. For moderate energy electrons ($E < 1$ MeV), the relativistic factor is $\gamma < 3$. The harmonic number n is equal to -1 for the first-order cyclotron resonance and $n = 0$ for Landau (or Cherenkov) resonance. For parallel wave propagation ($k_{||} = k$) the first-order cyclotron resonance is the most easily accessible: $\omega = kv_{||} + \Omega_c/\gamma$ (see comparison of Landau and cyclotron resonances in *Bell* [1986] and *Shklyar and Matsumoto* [2009, and references therein]). Because $\Omega_c > \omega$ particles should move in the direction opposite to the wave ($kv_{||}$<0) to satisfy the resonance condition. Therefore, many studies were devoted to particle trapping via first-order cyclotron resonance by an oppositely propagating wave: the interaction of electrons with lightning-generated whistler waves was considered by *Lauben et al.* [2001] and *Trakhtengerts et al.* [2003] and the interaction of electrons coming back from mirror points with whistlers generated at the equator was described by *Omura et al.* [2007] and *Bortnik et al.* [2008].

For oblique waves, $k_{||}$ can be substantially smaller than k. Thus, Landau resonance ($n = 0$) can be available when $\omega = k_{||}v_{||} > 0$. In this case, particles must propagate in the same direction as the wave. A classical scenario for Landau resonant interaction consists in particle trapping in the vicinity of the equator and escape from the resonance at high latitudes. *Shklyar and Matsumoto* [2009] estimate the energy gain for such a scenario in the case of nonrelativistic particles as $\sim\mu\Delta B - m_e(\omega^2/k_{||}^3)\Delta k_{||}$, where μ is the electron magnetic moment, m_e is electron mass, and ΔB and $\Delta k_{||}$ are difference of magnetic field amplitude and parallel wave number between points of trapping and escape. The energy gain corresponds to an increase of the magnetic field (some analog of the betatron mechanism) and a decrease of parallel wave vector (during wave propagation from the equator, $k_{||}$ decreases) [see, e.g., *Shklyar et al.*, 2004; *Breuillard et al.*, 2012].

While nonlinear acceleration via trapping into first-order cyclotron resonance has been described in detail in many papers [*Shklyar*, 1981; *Bell*, 1984; *Solovev and Shkliar*, 1986; *Roth et al.*, 1999; *Albert*, 1993; *Trakhtengerts*

et al., 2003; *Omura et al.*, 2007; *Bortnik et al.*, 2008; *Zheng et al.*, 2012], only few studies have considered nonlinear acceleration via trapping into Landau resonance for very oblique whistler waves [*Inan and Tkalcevic*, 1982; *Bell*, 1986; *Shklyar and Matsumoto*, 2009; *Artemyev et al.*, 2012b]. However, we have noted above that oblique chorus waves can be extremely intense, the recorded amplitude of their parallel electric field reaching 20 to 100 mV/m. Thus, the effects of Landau resonance with such waves deserve to be studied carefully. To this aim, we start by formulating a simplified model of the wave magnetic and electric fields, based on a detailed study by *Tao and Bortnik* [2010]. We assume wave propagation at an angle $\theta = \arccos(a\omega/\Omega_c)$ (for $a = 2$, one obtains a rough approximation for the Gendrin angle [*Gendrin*, 1961], and for $a = 1$, one gets a rough approximation for the resonance cone angle). We further obtain simplified expressions of $k_\parallel$ as a function of the background magnetic field: for propagation at the Gendrin angle, one has $k_\parallel \sim \Omega_c^{-1}$ while at the resonance cone $k_\parallel \sim \Omega_c^{-2}$ (see Appendix A). Moreover, it is worth noting that propagation at the Gendrin angle yields an almost constant normalized wave number $k \sim$ const for a nearly constant plasma frequency along geomagnetic field lines up to latitudes $\lambda = 30°$ to $40°$ where particles escape from resonance. Actually, *Denton et al.* [2006] have shown (based on Polar Plasma Wave Investigation (PWI) and CRRES Plasma Wave Experiment (PWE) data) that in the domain $L \in [5, 7]$, the plasma frequency ($\sim$ square root of plasma density) generally increases only by a factor $\sim$1.3–1.5 between the equator and $\lambda \sim 30°$ and by a factor $\sim$1.7–2.2 between the equator and $\lambda \sim 40°$. For the sake of simplicity (and since these variations remain small for $\lambda \leq 30°$), we shall hereafter consider a constant density over the considered latitudinal ranges in the analytical and numerical calculations. Nevertheless, the effects of a more realistic latitude-varying density will be assessed in the last section.

Next, a simple analytical model of electron acceleration via Landau resonance with an oblique whistler wave is formulated, considering a single trapping-escape event of a particle. The system geometry is such that the z direction is along the background dipolar magnetic field. Particles trapped into Landau resonance move with the wave at a resonant velocity $v_R(s) \approx \omega/k_\parallel(s)$ where s is the coordinate along the geomagnetic field line (i.e., $s = R_0 \int_0^s \sqrt{1 + 3\sin^2\lambda}\cos\lambda \mathrm{d}\lambda$ with $R_0 = R_E L$).

When considering Landau resonance, the particle moves along with the wave in such a way that its magnetic moment μ is conserved. In this case, the Hamiltonian of relativistic electrons with charge $-e$ and mass m_e can be written as

$$H = \sqrt{m_e^2 c^4 + c^2 p_\parallel^2 + c^2 m_e \mu B_{\mathrm{eq}} b(s)} - e\Phi(s, t),$$

where $(s, p_\parallel)$ are conjugate Hamiltonian variables representing, respectively, the parallel coordinate and momentum of particles. The magnitude of the background magnetic field is $B_{\mathrm{eq}} b(s)$ with an equatorial value B_{eq}, and the scalar potential of the wave is $\Phi(s, t)$ (i.e., the wave electric field is $E_\parallel = -\partial\Phi/\partial s$). For simplicity, we further consider a plane wave with an electrostatic component $E_\parallel = E(s)\cos\phi$ where wave phase ϕ can be defined as

$$\phi = \int^s k_\parallel(s)\mathrm{d}s - \omega t.$$

Here the perpendicular components of the wave electromagnetic field are neglected and we also assume conservation of the particle's magnetic moment. This is justified when considering Landau resonance (the perpendicular components of the wave electromagnetic field are important only for cyclotron resonances) [see *Shklyar and Matsumoto*, 2009].

The quasi-electrostatic mode of whistler waves corresponds to a simple approximation where the wave can be described by the scalar potential $\Phi = \Phi_0(s)\sin\phi$ with an amplitude $\Phi_0(s)$. Thus, the wave amplitude can be written as $E_\parallel \approx \Phi_0(s)k_\parallel(s) \approx E_0\cos\theta$, with θ the angle between the wave propagation direction and the background magnetic field. After introducing the dimensionless parameter $h = \mu B_{\mathrm{eq}}/m_e c^2$ and dimensionless momentum $p_\parallel \to p_\parallel/m_e c$, the equations of electron motion can be written as

$$\begin{cases} \gamma &= \sqrt{1 + p_\parallel^2 + hb(s)}, \\ \gamma\dot{s} &= cp_\parallel, \\ \dot{p}_\parallel &= -\frac{ch}{\gamma}\frac{\partial b(s)}{\partial s} - \frac{eE_0}{m_e c}\cos\theta\cos\phi, \\ \phi &= \int_0^s k(s')\cos\theta(s')\mathrm{d}s' - \omega t. \end{cases}$$

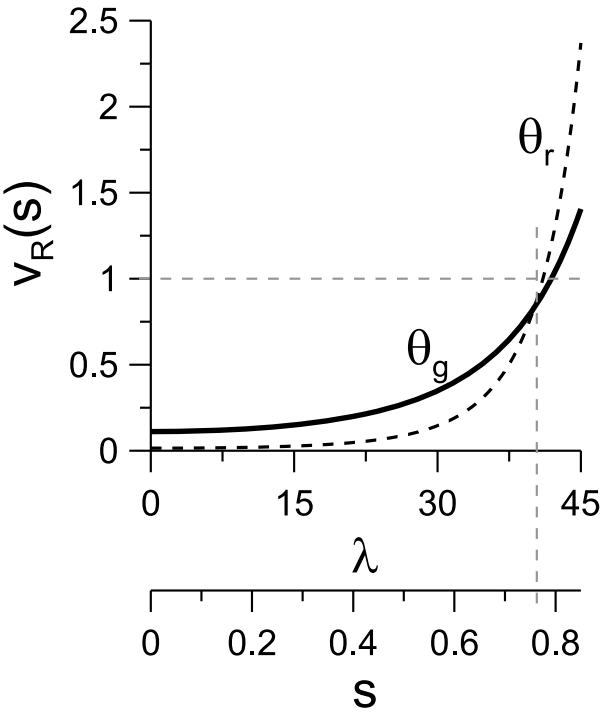

Figure 4. Profile of $v_R(s)$.

We further use the spatial scale $R_0 = LR_E$ to introduce the dimensionless coordinates $s \to s/R_0$ and $k \to kR_0$. The corresponding dimensionless time is $t \to tc/R_0$. We also use the expression $\cos\theta = a\omega/\Omega_{c,eq}b(s)$:

$$\begin{cases} \gamma &= \sqrt{1 + p_\parallel^2 + hb(s)}, \\ \gamma\dot{s} &= p_\parallel, \\ \dot{p}_\parallel &= -\frac{h}{\gamma}\frac{\partial b(s)}{\partial s} - \frac{eE_0R_0a\omega}{c^2m_e\Omega_{c,eq}}\frac{1}{b(s)}\cos\phi, \\ \phi &= \frac{\omega a}{\Omega_{c,eq}}\int_0^s \frac{k(s')}{b(s')}ds' - \frac{\omega R_0}{c}t. \end{cases}$$

With dimensionless parameters $\varepsilon = (eE_0R_0/m_ec^2)a$ and $\omega_m = \omega/\Omega_{c,eq}$ corresponding respectively to the normalized amplitude of the wave electric field and to the normalized wave frequency, one finds

$$\begin{cases} \gamma &= \sqrt{1 + p_\parallel^2 + hb(s)}, \\ \gamma\dot{s} &= p_\parallel, \\ \dot{p}_\parallel &= -\frac{h}{\gamma}\frac{\partial b(s)}{\partial s} - \varepsilon\omega_m\frac{1}{b(s)}\cos\phi, \\ \phi &= \omega_m\frac{R_0\Omega_{c,eq}}{c}\left(\frac{ca}{R_0\Omega_{c,eq}}\int_0^s \frac{k(s')}{b(s')}ds' - t\right). \end{cases}$$

For propagation at the resonance cone and Gendrin angles, we have

$$k \approx \frac{R_0\Omega_{c,eq}}{c}\frac{\Omega_{pe}}{\Omega_{c,eq}}\begin{cases} \frac{\omega_m}{\sqrt{\theta b(s)}}, & \theta = \theta_r, \\ 1, & \theta = \theta_g, \end{cases}$$

where $\eta = m_e/m_i$ is the electron to (effective) ion mass ratio. The corresponding wave phase is

$$\phi = k_0\begin{cases} \frac{\omega_m\omega_{pe}}{\sqrt{\eta}}\int_0^s \frac{ds'}{b^2(s')} - t, & \theta = \theta_r, \\ 2\omega_{pe}\int_0^s \frac{ds'}{b(s')} - t, & \theta = \theta_g, \end{cases}$$

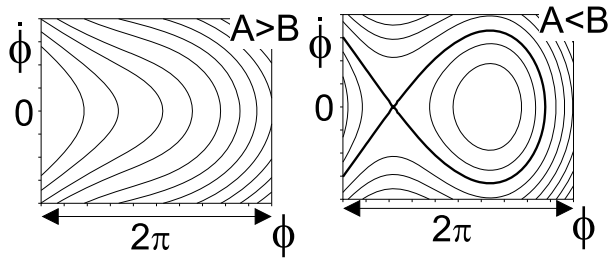

Figure 5. Phase portrait of the system (3).

where $k_0 = R_0\Omega_{c,eq}\omega_m/c$ and $\omega_{pe} = \Omega_{pe}/\Omega_{c,eq}$. Here a constant plasma density ω_{pe} = const has been assumed to simplify the following analytical estimates. Detailed justifications for this assumption are given below in section 5 and more specifically in Appendix B.

In the vicinity of the Landau resonance $\dot{\phi} = 0$, one has

$$\begin{cases} \omega_m\omega_{pe}\dot{s} = \sqrt{\eta}b^2(s), \ \theta = \theta_r, \\ 2\omega_{pe}\dot{s} \quad = b(s), \ \theta = \theta_g. \end{cases}$$

Now, we introduce the resonant velocity $v_R = 1/K(s)$ where

$$K_r = \frac{\omega_m\omega_{pe}}{\sqrt{\eta}}\frac{1}{b^2(s)}, \quad K_g = \frac{2\omega_{pe}}{b(s)}. \tag{1}$$

where subscripts r and g correspond respectively to the resonance cone and Gendrin angles.

Profiles of $v_R(s)$ for these two angles of propagation are displayed in Figure 4. One can see that the normalized resonant velocity $v_R \ll 1$ at small latitudes. However, v_R becomes close to one in the vicinity of $\lambda = 40°$. There, the wave phase velocity actually approaches the speed of light. Thus, our approximations are not

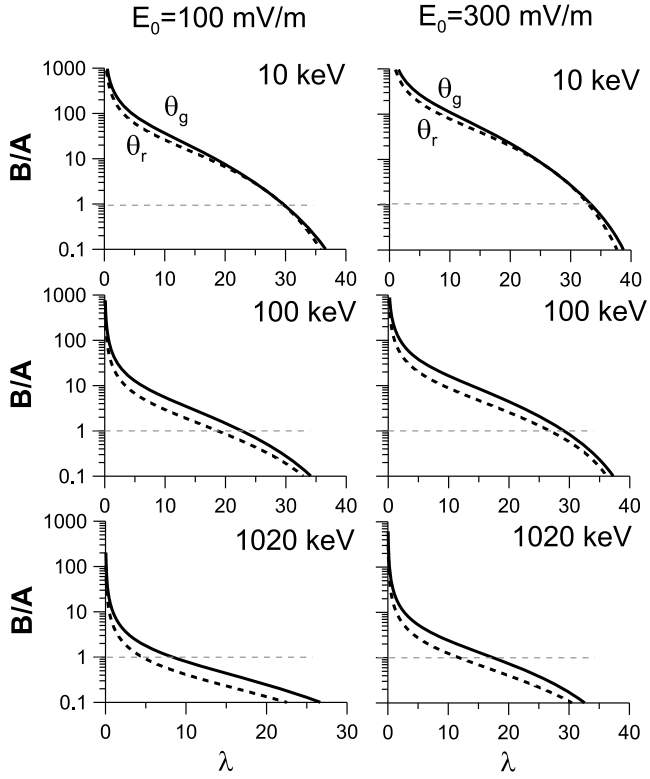

Figure 6. Profiles of ratio A/B for $\theta = \theta_g$ and $\theta = \theta_r$. Three different values of the initial electron energy and two values of the wave electric field amplitude are considered.

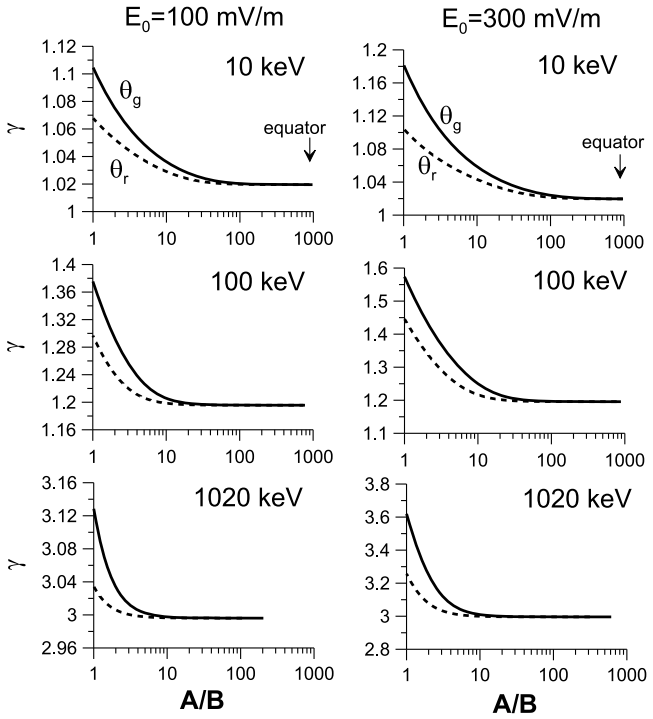

Figure 7. Energy of resonant electrons as a function of the ratio A/B for $\theta = \theta_g$ and $\theta = \theta_r$. Three different values of the initial electron energy and two values of the wave electric field amplitude are considered.

valid anymore. Particles should therefore escape from resonance somewhere before the wave phase velocity becomes too large.

In the vicinity of resonance, we can write $p_\parallel = v_R\gamma$ and $\gamma = \gamma_R\sqrt{1+hb(s)}$ with $\gamma_R = (1-v_R^2)^{-1/2}$. The equation for s can be rewritten as $\gamma\ddot{s} + \dot{\gamma}v_R = \dot{p}_\parallel$. Using the expression for γ, the first derivative of the parallel momentum can now be written as

$$\dot{p}_\parallel = \gamma\ddot{s} + \gamma_R^2\left(\frac{h}{\gamma}\frac{\partial b(s)}{\partial s}v_R + \gamma v_R^2\frac{\partial v_R}{\partial s}\right)v_R.$$

Moreover, the second derivative of the phase ϕ gives

$$\ddot{\phi} = k_0\left(\ddot{s}K(s) + v_R^2\frac{\partial K(s)}{\partial s}\right) = k_0\left(\frac{\ddot{s}}{v_R} - \frac{\partial v_R}{\partial s}\right).$$

As a result, we obtain

$$\dot{p}_\parallel = v_R\gamma\ddot{\phi}/k_0 + \gamma_R^2 v_R\gamma\frac{\partial v_R}{\partial s} + \gamma_R^2 v_R^2\frac{h}{\gamma}\frac{\partial b(s)}{\partial s}.$$

Substituting this expression into the equation for $p_\parallel$, we finally get

$$\begin{cases} \gamma\ddot{\phi} &= -\frac{k_0}{v_R}(\mathrm{A}(s) + \mathrm{B}(s)\cos\phi), \\ \mathrm{A}(s) &= \frac{\gamma_R^2 h}{\gamma}\frac{\partial b(s)}{\partial s} + \gamma\gamma_R^2\frac{1}{2}\frac{\partial v_R^2}{\partial s}, \\ \mathrm{B}(s) &= \frac{\varepsilon\omega_m}{b(s)}. \end{cases} \quad (2)$$

The corresponding Hamiltonian of this system is

$$H_\phi = \frac{1}{2}\gamma\dot{\phi}^2 + \frac{k_0}{v_R}(\mathrm{A}(s) + \mathrm{B}(s)\sin\phi). \quad (3)$$

This is the classical Hamiltonian of the nonlinear pendulum, with well-known phase portrait (Figure 5) [see *Shklyar and Matsumoto*, 2009; *Artemyev et al.*, 2012b, and references therein]. For A < B, one can find a region filled with closed trajectories in the phase plane $(\phi, \gamma\dot{\phi})$. Resonant particles move along these trajectories with a corresponding oscillation around $\dot{\phi} = 0$. Thus, trapping into the Landau resonance is possible if the wave amplitude is large enough to get A < B.

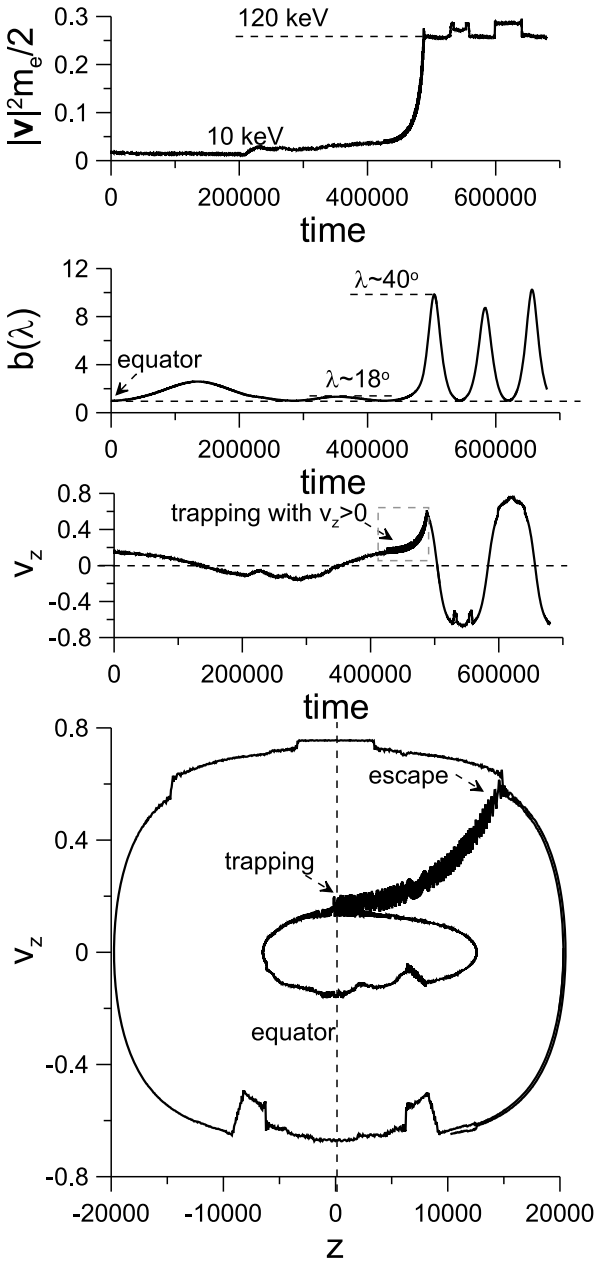

Figure 8. Particle trajectory for a 10 keV electron. The initial pitch angle is ~31.7° and $E_{||} \sim 75$ mV/m (see Appendix A). (from top to bottom) Energy as function of time, z component of the dipole magnetic field along the trajectory, z component of particle velocity, and particle trajectory in (z, v_z) plane. Moments of trapping and escape are indicated by arrows. Coordinates are normalized to $c/\Omega_{c,eq}$; time is normalized to $\Omega_{c,eq}$; and velocities are normalized to the speed of light c.

Consequently, to determine the possible regions of resonant acceleration, one needs to compare the relative magnitudes of the terms A and B along the field lines [see *Bell*, 1986; *Artemyev et al.*, 2012b, and references therein]. Simple analytical estimates can be derived for the region far from $\lambda \sim 40°$ where we can set $\gamma_R \approx 1$. In this case, the equation A = B gives

$$\begin{cases} \frac{\varepsilon\omega_m}{b(s)} = \left(\frac{h}{\gamma} + \gamma\frac{b(s)}{(2\omega_{pe})^2}\right)\frac{\partial b(s)}{\partial s}, \ \theta = \theta_g, \\ \frac{\varepsilon\omega_m}{b(s)} = \left(\frac{h}{\gamma} + \gamma\frac{2\eta b^3(s)}{(\omega_m\omega_{pe})^2}\right)\frac{\partial b(s)}{\partial s}, \ \theta = \theta_r, \end{cases}$$

where $\gamma \approx \sqrt{1 + hb(s)}$. For $b < \omega_{pe}^2$ (i.e., $\lambda < 40°$), we can neglect the second term in these equations. Therefore, the particle acceleration is then determined by the magnetic field inhomogeneity (the same conclusion

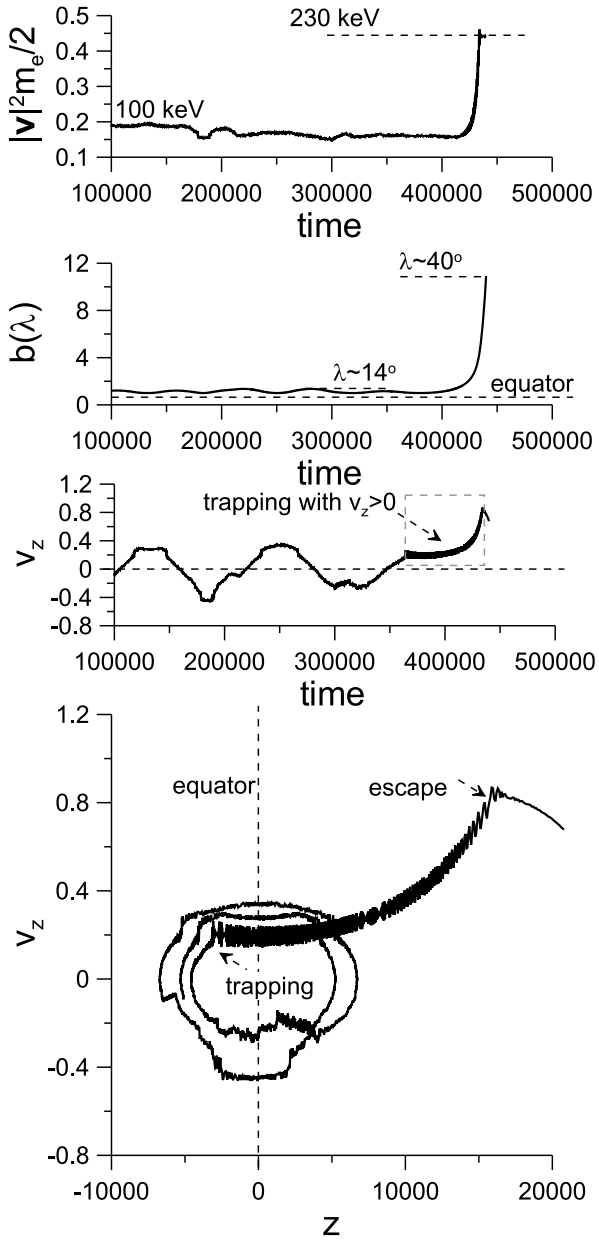

Figure 9. The same as in Figure 8 but for 100 keV electron (here the initial pitch angle is ~68.3°).

was reached by *Artemyev et al.* [2012b]). In this case, the critical (minimum) level of the wave amplitude required for nonlinear interaction is given by

$$\varepsilon = \frac{h}{2\gamma\omega_m}\frac{\partial b^2}{\partial s}. \tag{4}$$

Thus, to get trapped in the vicinity of the equator (where $\lambda < 10°$ and $(\partial b^2/\partial s) \sim 1.5$), a particle needs to interact with a wave of high-enough amplitude $E_0 > E_{cr}$, where the critical amplitude E_{cr} reads as

$$E_{cr}[\mathrm{mV/m}] \sim \frac{60\ \sin^2\alpha_{eq}}{a\ L\ \omega_m} \tag{5}$$

with α_{eq} the electron equatorial pitch angle. For $L \sim 5$, $\omega_m \sim 0.35$ typically, and $\alpha_{eq} \sim 30° - 60°$, the corresponding critical value of the wave amplitude given by equation (5) is $E_{cr} \sim 10$–25 mV/m close to the resonance cone and twice less near the Gendrin angle.

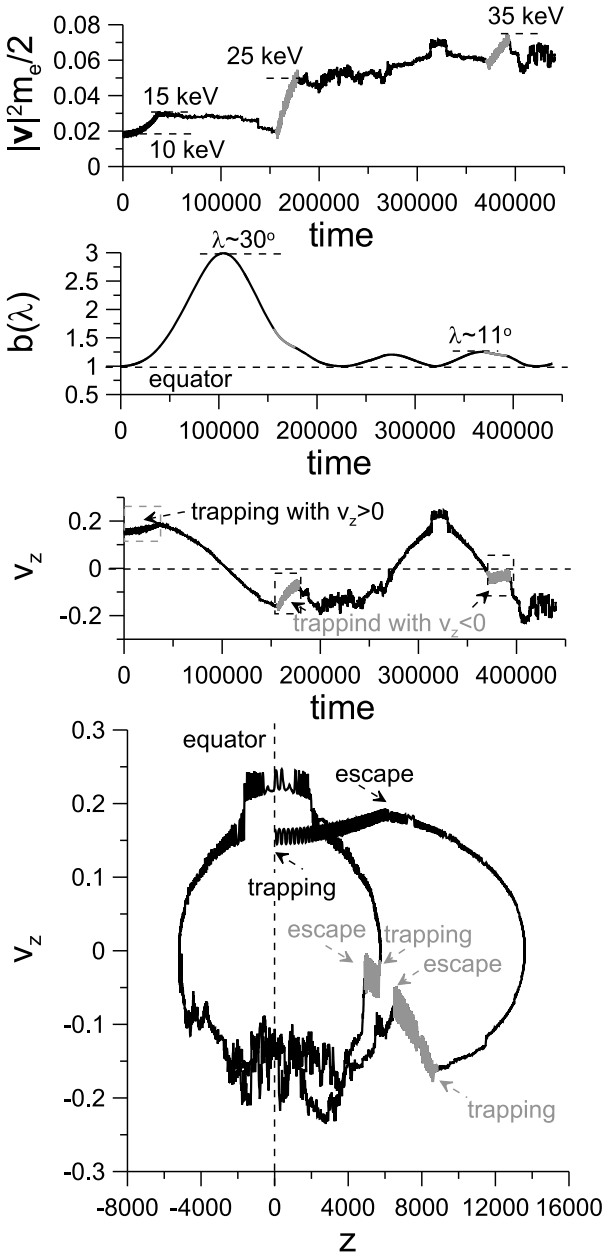

Figure 10. The same as in Figure 8 but for another initial pitch angle ~33.4°. Grey color shows fragment of trajectory where particle is trapped into first-order cyclotron resonance.

Profiles of B/A are shown in Figure 6 for several values of initial electron energy. Here the initial equatorial pitch angle α_{eq} is obtained by assuming that the resonance condition is satisfied at the equator for a given energy or γ value:

$$\cos\alpha_{eq} = K_{eq}^{-1}(1-\gamma^{-2})^{-1/2},$$
$$K_{eq} = \omega_{pe}\begin{cases} \omega_m/\sqrt{\eta}, & \theta=\theta_r, \\ 2, & \theta=\theta_g. \end{cases}$$

For 10–100 keV electrons, the ratio B/A becomes smaller than 1 for $\lambda > 25° - 35°$ (for both angles of wave propagation $\theta = \theta_g$ and $\theta = \theta_r$). In the vicinity of $\lambda \sim 30°$ (where B/A $\approx$ 1), particles should therefore escape from the resonance, because the Hamiltonian (3) phase portrait does not contain any region with trapped trajectories anymore. Note that an increase of particle energy results in a decrease of the latitude of escape where B/A $\approx$ 1.

Finally, the maximum energy gain before escape from the resonance can be estimated by plotting $\gamma=\gamma_R\sqrt{1+hb(s)}$ as a function of the ratio B/A (see Figure 7). A large value of B/A $\gg$ 1 corresponds to the nearly equatorial region where particles can be trapped by the waves. The location where B/A $\approx$ 1 corresponds to escape. It is worth noting that the energy gain is larger for resonance with waves propagating at θ_g as compared to θ_r. For 10 keV electrons interacting with 100 mV/m waves, the maximum possible energy is $\gamma \approx 1.1$; i.e., the corresponding maximum energy gain is ~50 keV. For 100 keV and 1 MeV electrons, we obtain an energy gain of 50–100 keV. This energy gain increases for higher wave amplitude (see Figure 7, right)

To illustrate this process of electron acceleration by Landau resonance with very oblique chorus waves and to provide some comparisons with analytical estimates, a few test-particle simulations have been performed, using typically measured parameters (see the description of the numerical scheme in Appendix A). A typical electron acceleration in Landau resonance for $E = 10$ keV is shown in Figure 8. One can see that the particle is trapped with a positive v_z component of velocity, as expected for the Landau resonance. Here the wave travels with the trapped particle up to $\lambda \sim 40°$. The corresponding energy gain is ~100 keV, i.e., this gain is much larger than the initial energy of the particle. The particle trajectory in the (z, v_z) plane contains quasi-closed circles corresponding to classical bounce oscillations between high-latitude mirror points. The trapped motion corresponds to a fragment of trajectory with increasing v_z and z. In addition, electron trapping into Landau resonance corresponds to a decrease of the particle pitch angle (and a corresponding increase of the amplitude of bounce oscillations). An example of a 100 keV electron trajectory is shown in Figure 9. Trapping into Landau resonance (with positive v_z) results again in a significant energy gain ~130 keV. Here it is worth mentioning that particle trajectories where obtained with full 3-D wave electromagnetic fields. The close similarity between analytically predicted and test-particle energy gains lends further credibility to our analytical estimates based on the quasi-electrostatic approximation.

5. Discussion

In this paper, we present and analyze a model of nonlinear electron acceleration via Landau resonance with an oblique high-amplitude whistler mode wave. This model can be considered as a generalization of the simplified model proposed by *Artemyev et al.* [2012b]. We only consider Landau resonance when the particle travels with the wave and gains energy due to the inhomogeneity of the background magnetic field along its trajectory. Most of the parallel energy increase is then stored away under the form of perpendicular energy due to conservation of the first adiabatic invariant during particle motion toward higher latitudes. In our numerical simulations, however, the effects of the first-order cyclotron resonance can also be observed when the particle moves in the direction opposite to the wave. An example of such a trajectory is shown in Figure 10. In this figure, the effects of both the Landau and first-order cyclotron resonances are plain to see. In the vicinity of the equator, the particle becomes trapped into Landau resonance and gains ~5 keV. Then, first-order cyclotron resonance occurs after bounce from the mirror point and the particle gains an additional ~10 keV (after that, yet another first-order cyclotron resonance interaction takes place). One can see that the profile of energy growth with time differs for the Landau and the first-order cyclotron resonances (compare also with Figures 8 and 9). Similar profiles of energy growth for first-order cyclotron resonance were already obtained by *Bortnik et al.* [2008], *Tao et al.* [2012], and *Zheng et al.* [2012]. Here we have deliberately restricted our analytical estimates to the case of the sole Landau resonance, leaving a detailed description of the effects of first-order cyclotron resonance with very oblique waves for further publications (some preliminary comparison of these two resonances can be found in *Artemyev et al.* [2013]).

It is worth noting that in our test-particles simulations, a simplified model of plane wave has been used instead of considering an actual wave packet with finite sizes (length along the direction of propagation and width across field lines). The effect of wave localization along field line for the Landau resonance was considered by *Artemyev et al.* [2012b] and for the first-order cyclotron resonance by *Tao et al.* [2012]. For first-order cyclotron resonance, this effect can play a critical role, because the particle moves in a direction opposite to the wave. Thus, the duration of wave-particle interaction is limited by the length of the wave packet (or by the inhomogeneity of the background magnetic field for wide enough wave packet). For Landau resonance, this effect is not so essential because the particle moves with one particular wave inside the wave packet. As a result, acceleration is not influenced substantially by the length of the wave packet. However, in the case of Landau resonance, it is important that the wave packet conserves its length during the propagation. According to Polar data, the number of separate, coherent waves inside a particular wave packet decreases

with increasing magnetic latitude [*Tsurutani et al.*, 2011]. This effect can result in a decrease of the efficiency of electron acceleration due to Landau resonance (see estimates in *Artemyev et al.* [2012b]). The finite width of wave packets across the field lines [*Agapitov et al.*, 2011a] can also play an important role for resonant trapping (see discussion in *Artemyev et al.* [2012b]).

Besides, a highly efficient process of resonant particle acceleration should lead to rapid wave damping due to conservation of energy. Wave damping is known to be more effective for very oblique waves propagating near the resonance cone than for less oblique waves, due to the smaller parallel phase velocity [e.g., *Bortnik et al.*, 2006]. Therefore, some additional mechanism is required for supporting high-amplitude whistler waves. Such a mechanism was actually considered by *Shklyar* [2011a]. It was shown that some gain of energy by resonantly trapped particles can be compensated by a loss of energy by transient particles. A fine balance results in the conservation of wave energy. In such a system, the wave can be considered as a mediator of energy transfer between two particle populations (transient and trapped), provided that the total wave energy is substantially smaller than the available energy of both these populations [*Shklyar*, 2011b]. However, wave damping is likely to prevail at high latitudes, because particle acceleration should be more efficient than wave amplification in this region.

In the above calculations, the dispersion relation for whistler mode waves has been derived in the cold plasma limit. While finite temperature effects remain small when these waves propagate not too close to the resonance cone (for instance near the Gendrin angle), it is well known that the dispersion is modified in the very close vicinity of the resonance cone angle in a warm plasma (i.e., for bulk plasma temperature $T_e \geq 1$eV), mitigating the variation of the refractive index and allowing waves to propagate at angles larger than the resonance cone angle [*Hashimoto et al.*, 1977]. Although interesting and potentially important, these effects have not been considered in the present study, which rather covers the whole wave normal angle range comprised between the Gendrin and resonance cone angles. Warm plasma effects should mainly reduce the wave number variation as a function of wave normal angle very close to the resonance cone, making it somewhat intermediary between cold plasma results at the resonance cone and at the Gendrin angle.

Finally, we have also used here the approximation of a constant plasma frequency along geomagnetic field lines. It allows for more simple analytical estimates. However, a finite variation of the plasma density with latitude has been observed [*Denton et al.*, 2006]. Such a variation can be important for quasi-linear scattering of particles [*Summers and Ni*, 2008; *Artemyev et al.*, 2012a]. To describe the corresponding variation of $\Omega_{pe}(\lambda)$, we therefore introduce the parameter $\chi < 1$, assuming that $\Omega_{pe} \sim \Omega_c^{\chi}$. Based on the study by *Denton et al.* [2006] of Polar PWI and CRRES PWE data, the outer belt plasma density over latitude ranges $0°<\lambda<30°$ and $0°<\lambda<40°$ (corresponding to the considered particle acceleration ranges) may generally be fitted by power laws such that $\Omega_{pe}^2 \sim \cos^{-\kappa}\lambda$ with $\kappa \sim 4$ to 6, corresponding to $\chi \sim 0.25$–0.4. The effect of such a variation of Ω_{pe} on particle acceleration via Landau resonance has been investigated in Appendix B for waves propagating near the Gendrin angle (representative of most of the large wave normal angle range, except for the very close vicinity of the resonance cone). It is interesting to note that the increase of plasma density with latitude results in an increase of the latitude at which particles should escape from resonance (this effect is especially well pronounced for small energy particles). However, the total energy gain actually remains the same as in the constant plasma density case, because the additional energy gain is almost fully compensated by energy losses due to the decrease of the resonant velocity $v_R \sim \Omega_c^{1-\chi}$ (see Appendix B for more details). Therefore, even a relatively strong variation of the plasma density (for $\chi = 0.4$) does not change substantially the efficiency of particle acceleration by very oblique waves, provided that these waves are not propagating too close to the resonance cone.

6. Conclusions

In this paper, we have presented 15 selected THEMIS observations of high-amplitude whistler waves. The main properties of these waves are as follows.

1. Waves often propagate at a large angle $\theta \in [\theta_g, \theta_r]$ relative to the background magnetic field (even in the vicinity of the magnetic equator).
2. Due to the large angle of wave propagation, the wave polarization is substantially noncircular. Most of the observed waves propagate in the quasi-electrostatic mode, with a high-amplitude electric field (> 50 mV/m).
3. The component of the wave electric field along the background magnetic field is about 25%–75% of the total wave amplitude (~20–50 mV/m).

The measured parameters of high-amplitude oblique chorus waves have then been used to investigate an eventual nonlinear acceleration of electrons by Landau resonance with these waves, both analytically and by means of numerical simulations. The corresponding results are as follows:

1. The large parallel component of the wave electric field waves can trap electrons into Landau resonance at low to medium latitudes. This trapping results in an energy gain in the dipolar magnetic field of up to 100 keV during one bounce period.
2. Acceleration in the Landau resonance is more effective for electrons with low initial energy ~10 keV (corresponding to typical plasma sheet electron energies) and for wave propagation near the Gendrin angle. The energy of accelerated electrons can increase by up to 1 order of magnitude.
3. Acceleration in the Landau resonance is associated with a substantial decrease of electron equatorial pitch angle and, as a result, can lead to fast particle precipitation. Actually, a correlation between high-amplitude whistler waves and bursty precipitations has often been observed [*Thorne et al.*, 2005; *Kersten et al.*, 2011; *Lyons et al.*, 2012; *Panov et al.*, 2013].

Appendix A: Test-Particle Trajectories

In this appendix, we describe the distribution of the wave electromagnetic field and the scheme of calculation of trajectories of test particles. We consider a background magnetic field using a simplified dipole model [see *Bell*, 1984]: $\mathbf{B}_0 = B_z(\lambda)\mathbf{e}_z + B_x(\lambda, x)\mathbf{e}_x$ where $B_z = B_{eq}\sqrt{1+3\sin^2\lambda}/\cos^6\lambda$ and $B_x = -x(dB_z/d\lambda)(d\lambda/dz)$ (i.e., condition $div\mathbf{B} = 0$ is satisfied). In such field geometry the z axis corresponds to the direction along the geomagnetic field. The distribution of the components of the wave electromagnetic field along a geomagnetic field line for obliquely propagating waves is given in *Tao and Bortnik* [2010].

For a sufficiently large ratio of plasma frequency to gyrofrequency $\Omega_{pe}/\Omega_c \gg 1$ [see *Ginzburg and Rukhadze*, 1975], the cold plasma dispersion relation of whistler mode waves can be written as

$$\omega^2 = \frac{\Omega_c^2\cos^2\theta}{(1+(\Omega_{pe}/kc)^2)^2} + \frac{\eta\Omega_c^2}{1+(\Omega_{pe}/kc)^2},$$

where $\eta = m_e/m_i$ and m_i is the effective mass of the ion mixture. We also introduce $\Omega_{c,eq}$ as the value of Ω_c evaluated at the equator. From this expression one can easily obtain

$$(kc)^2 = \Omega_{pe}^2\frac{2\cos^2\theta_r}{\eta - 2\cos^2\theta_r + \sqrt{\eta^2+4\cos^2\theta\cos^2\theta_r}},$$

where $\cos\theta_r = \omega/\Omega_c$. As a result, if we assume wave propagation with a certain angle $\theta = \theta(\lambda)$ we can obtain the distribution of all the components of the wave electromagnetic field [*Tao and Bortnik*, 2010].

Let us also mention two important properties of the variation of k as a function of latitude for wave propagation with resonance cone θ_r and Gendrin θ_g angles. Due to the smallness of $\eta \ll 1$ we can use the expansion

$$(kc)^2 \approx \Omega_{pe}^2\frac{\cos^2\theta_r}{\frac{1}{2}\eta + \cos\theta\cos\theta_r - \cos^2\theta_r}.$$

Then for $\cos\theta = \cos\theta_r$ we have

$$(kc)^2 \approx \frac{2\Omega_{pe}^2\cos^2\theta_r}{\eta} = \frac{2\Omega_{pe}^2\omega^2}{\eta\Omega_c^2}.$$

For Gendrin angle $\cos\theta = 2\omega/\Omega_c$ we get

$$(kc)^2 \approx \Omega_{pe}^2\frac{\cos^2\theta_r}{\frac{1}{2}\eta + \cos^2\theta_r} \approx \Omega_{pe}^2.$$

We consider oblique waves with $\theta = \arccos(2\omega/\Omega_c)$. In this case

$$k\cos\theta = \frac{2\Omega_{pe}\omega}{c\Omega_c} = \frac{2}{R_0}\chi\omega_{pe}\omega_m\frac{\Omega_{c,eq}}{\Omega_c},$$
$$k\sin\theta = k\sqrt{1-\cos^2\theta} \approx \frac{1}{R_0}\chi\omega_{pe},$$

where $R_0 = R_E L$, $\omega_m = \omega/\Omega_{c,eq}$, $\omega_{pe} = \Omega_{pe}/\Omega_{c,eq}$, and $\chi = R_0\Omega_{c,eq}/c$. In this case the wave phase has a form

$$\frac{d\phi}{dt} = 2\frac{v_z}{R_0}\chi\omega_{pe}\omega_m\frac{\Omega_{c,eq}}{\Omega_c} + \frac{v_x}{R_0}\chi\omega_{pe} - \omega.$$

Equations of motion of nonrelativistic electrons with charge $-e$ and mass m_e in the electromagnetic fields have the form

$$m_e\dot{\mathbf{v}} = -e\mathbf{E}_w - \frac{e}{c}\left[\mathbf{v}\times(\mathbf{B}_w + \mathbf{B}_0)\right],\ \dot{\mathbf{r}} = \mathbf{v}.$$

We introduce dimensionless parameters and variables $t \to t\Omega_{c,eq}$, $\mathbf{r} \to \mathbf{r}\Omega_{c,eq}/c$, $\mathbf{v} \to \mathbf{v}/c$, giving

$$\begin{cases} \dot{\mathbf{v}} = -\tilde{\mathbf{E}}_w - [\mathbf{v}\times(\tilde{\mathbf{B}}_w + \tilde{\mathbf{B}}_0)],\ \dot{\mathbf{r}} = \mathbf{v}, \\ \dot{\lambda} = v_z(d\lambda/dz) = v_z\left(\frac{\sqrt{1+3\sin^2\lambda}}{\chi\cos\lambda}\right), \\ \dot{\phi} = 2v_z\omega_{pe}\omega_m\frac{\cos^6\lambda}{\sqrt{1+3\sin^2\lambda}} + v_x\omega_{pe} - \omega_m, \\ \theta(\lambda) = \arccos\left(\frac{2\omega_m\cos^6\lambda}{\sqrt{1+3\sin^2\lambda}}\right), \end{cases}$$

and

$$\begin{cases} \tilde{\mathbf{E}}_w = \tilde{B}_{w,y}(\mathbf{E}_w/B_{w,y}), \quad \tilde{\mathbf{B}}_w = \tilde{B}_{w,y}(\mathbf{B}_w/B_{w,y}), \\ \tilde{\mathbf{B}}_0 = \frac{\sqrt{1+3\sin^2\lambda}}{\cos^6\lambda}\mathbf{e}_z - \frac{x}{\chi}\frac{3\sin\lambda(8-5\cos^2\lambda)}{\sqrt{(1+3\sin^2\lambda)}\cos^8\lambda}\mathbf{e}_x. \end{cases}$$

where $B_{w,y}$ is normalized so that the total wave energy is conserved during wave propagation. We consider 10–100 keV particles (initially $|\mathbf{v}| \approx 0.01$–$0.5$) interacting with the wave at $L = 4.5$ (where $B_{eq} \approx 330$ nT, $\Omega_{c,eq} \approx 6\cdot 10^4$ rad/s, and $\chi \approx 6\cdot 10^3$ rad). Wave frequency is $\omega_m = 0.35$; plasma frequency is $\omega_{pe} = 4.5$. For a total electric field amplitude $E_{w,0} = 300$ mV/m, the corresponding E_z component along the magnetic field line is about 75 mV/m.

Appendix B: Role of Plasma Density Variation

In this appendix, we consider the role of the variation of the plasma density (i.e., Ω_{pe}) with latitude λ. For the sake of simplicity, all the estimates are derived for waves propagating at the Gendrin angle. In this case, the wave number k varies with b and we can write the following expression for the dimensionless phase ϕ:

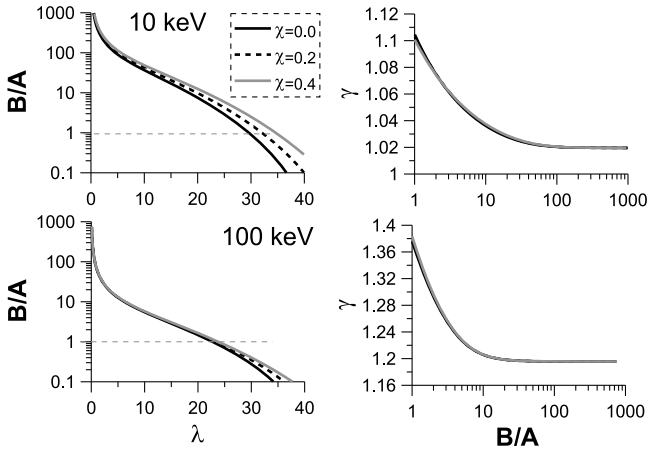

Figure B1. (left column) Profiles of ratio A/B and (right column) energy of resonant electron as function of ratio A/B for three values of χ. The electric field amplitude is 100 mV/m.

$$k \approx \frac{R_0\Omega_{c,\mathrm{eq}}}{c}\frac{\Omega_{\mathrm{pe,eq}}}{\Omega_{c,\mathrm{eq}}}b^{\chi},$$

$$\phi = 2k_0\omega_{\mathrm{pe}}\int_0^s \frac{\mathrm{d}s'}{b^{1-\chi}(s')} - t,$$

where we use the approximation $\Omega_{\mathrm{pe}} = \Omega_{\mathrm{pe,eq}}b^{\chi}$ with $\chi < 1$ (dimensionless parameters are as follows: $k_0 = R_0\Omega_{c,\mathrm{eq}}\omega_m/c$ and $\omega_{\mathrm{pe}} = \Omega_{\mathrm{pe}}/\Omega_{c,\mathrm{eq}}$). Landau resonance corresponds to $\dot{s} = v_R = 1/K(s)$ with $K(s) = 2\omega_{\mathrm{pe}}/b^{1-\chi}$. In comparison with the constant plasma density case, now the resonant velocity varies slower with b. Thus, particles can spend more time in resonance with the wave.

The dynamics of resonant phase ϕ can still be described by Hamiltonian (3) but with a new $K(s)$. Thus, we can plot the ratio B/A as a function of λ for systems with constant plasma density and for various χ values (see Figure B1, left column). The variation of the plasma density increases the latitude at which particles should escape from the resonance. This effect can be important for small initial energies, while almost negligible for 100 keV electrons. An increase of latitudes of escape results in an increase of the final value of b and, as a result, may lead to an increase of resonant energy $\gamma \sim \sqrt{1+hb}$. However, we have here a competition between two factors: an increase of b (corresponding to an increase of energy $\gamma \sim \sqrt{1+hb}$) and a decrease of $v_R \sim b^{1-\chi}$ (corresponding to a decrease of energy $\gamma \sim 1/\sqrt{1-v_R^2}$). Remarkably, these two effects almost compensate each other, so that the final energy gain appears to be nearly independent of χ (see Figure B1, right column).

Acknowledgments
This work was supported by CNES through the grant "Modeles d'ondes." Work of A.V.A. was also partially supported by the grant MK-1781.2014.2.

Robert Lysak thanks Paul J. Kellogg and an anonymous reviewer for their assistance in evaluating this paper.

References

Agapitov, O., V. Krasnoselskikh, T. Dudokde Wit, Y. Khotyaintsev, J. S. Pickett, O. Santolík, and G. Rolland (2011a), Multispacecraft observations of chorus emissions as a tool for the plasma density fluctuations' remote sensing, *J. Geophys. Res.*, *116*, A09222, doi:10.1029/2011JA016540.

Agapitov, O., V. Krasnoselskikh, Y. V. Khotyaintsev, and G. Rolland (2011b), A statistical study of the propagation characteristics of whistler waves observed by Cluster, *Geophys. Res. Lett.*, *382*, L20103, doi:10.1029/2011GL049597.

Agapitov, O., V. Krasnoselskikh, Y. V. Khotyaintsev, and G. Rolland (2012), Correction to "A statistical study of the propagation characteristics of whistler waves observed by Cluster", *Geophys. Res. Lett.*, *39*, L24102, doi:10.1029/2012GL054320.

Agapitov, O., A. Artemyev, V. Krasnoselskikh, Y. V. Khotyaintsev, D. Mourenas, H. Breuillard, M. Balikhin, and G. Rolland (2013), Statistics of whistler mode waves in the outer radiation belt: Cluster STAFF-SA measurements, *J. Geophys. Res. Space Physics*, *118*, 3407–3420, doi:10.1002/jgra.50312.

Albert, J. M. (1993), Cyclotron resonance in an inhomogeneous magnetic field, *Phys. Fluids B*, *5*, 2744–2750, doi:10.1063/1.860715.

Artemyev, A., O. Agapitov, H. Breuillard, V. Krasnoselskikh, and G. Rolland (2012a), Electron pitch-angle diffusion in radiation belts: The effects of whistler wave oblique propagation, *Geophys. Res. Lett.*, *39*, L08105, doi:10.1029/2012GL051393.

Artemyev, A., V. Krasnoselskikh, O. Agapitov, D. Mourenas, and G. Rolland (2012b), Non-diffusive resonant acceleration of electrons in the radiation belts, *Phys. Plasmas*, *19*, 122,901, doi:10.1063/1.4769726.

Artemyev, A. V., A. A. Vasiliev, D. Mourenas, O. Agapitov, and V. Krasnoselskikh (2013), Nonlinear electron acceleration by oblique whistler waves: Landau resonance vs. cyclotron resonance, *Phys. Plasmas*, *20*, 122,901, doi:10.1063/1.4836595.

Auster, H. U., et al. (2008), The THEMIS fluxgate magnetometer, *Space Sci. Rev.*, *141*, 235–264, doi:10.1007/s11214-008-9365-9.

Bell, T. F. (1965), Nonlinear Alfvén waves in a Vlasov plasma, *Phys. Fluids*, *8*, 1829–1839, doi:10.1063/1.1761115.

Bell, T. F. (1984), The nonlinear gyroresonance interaction between energetic electrons and coherent VLF waves propagating at an arbitrary angle with respect to the earth's magnetic field, *J. Geophys. Res.*, *89*, 905–918, doi:10.1029/JA089iA02p00905.

Bell, T. F. (1986), The wave magnetic field amplitude threshold for nonlinear trapping of energetic gyroresonant and Landau resonant electrons by nonducted VLF waves in the magnetosphere, *J. Geophys. Res.*, *91*, 4365–4379, doi:10.1029/JA091iA04p04365.

Bonnell, J. W., et al. (2008), The Eelectric field instrument (EFI) for THEMIS, *Space Sci. Rev.*, *141*, 303–341, doi:10.1007/s11214-008-9469-2.

Bortnik, J., U. S. Inan, and T. F. Bell (2006), Landau damping and resultant unidirectional propagation of chorus waves, *Geophys. Res. Lett.*, *33*, L03102, doi:10.1029/2005GL024553.

Bortnik, J., R. M. Thorne, and U. S. Inan (2008), Nonlinear interaction of energetic electrons with large amplitude chorus, *Geophys. Res. Lett.*, *35*, L21102, doi:10.1029/2008GL035500.

Bortnik, J., L. Chen, W. Li, R. M. Thorne, and R. B. Horne (2011), Modeling the evolution of chorus waves into plasmaspheric hiss, *J. Geophys. Res.*, *116*, A08221, doi:10.1029/2011JA016499.

Bourdarie, S., D. Boscher, T. Beutier, J.-A. Sauvaud, and M. Blanc (1996), Magnetic storm modeling in the Earth's electron belt by the Salammbô code, *J. Geophys. Res.*, *101*, 27,171–27,176, doi:10.1029/96JA02284.

Breuillard, H., Y. Zaliznyak, V. Krasnoselskikh, O. Agapitov, A. Artemyev, and G. Rolland (2012), Chorus wave-normal statistics in the Earths radiation belts from ray tracing technique, *Ann. Geophys.*, *30*, 1223–1233, doi:10.5194/angeo-30-1223-2012.

Cattell, C., et al. (2008), Discovery of very large amplitude whistler-mode waves in Earth's radiation belts, *Geophys. Res. Lett.*, *35*, L01105, doi:10.1029/2007GL032009.

Chen, L., R. M. Thorne, W. Li, and J. Bortnik (2013), Modeling the wave normal distribution of chorus waves, *J. Geophys. Res. Space Physics*, *118*, 1074–1088, doi:10.1029/2012JA018343.

Chum, J., O. Santolik, D. A. Gurnett, and J. S. Pickett (2009), Oblique lower band chorus waves: Time shifts between discrete elements observed by the Cluster spacecraft, *J. Geophys. Res.*, *114*, A00F02, doi:10.1029/2009JA014366.

Cully, C. M., J. W. Bonnell, and R. E. Ergun (2008), THEMIS observations of long-lived regions of large-amplitude whistler waves in the inner magnetosphere, *Geophys. Res. Lett.*, *35*, L17S16, doi:10.1029/2008GL033643.

Davydovskiĭ, V. Y. (1963), Possibility of resonance acceleration of charged particles by electromagnetic waves in a constant magnetic field, *Sov. Phys. JETP*, *16*, 629.
Demekhov, A. G., V. Y. Trakhtengerts, M. J. Rycroft, and D. Nunn (2006), Electron acceleration in the magnetosphere by whistler-mode waves of varying frequency, *Geomag. Aeron.*, *46*, 711–716, doi:10.1134/S0016793206060053.
Denton, R. E., K. Takahashi, I. A. Galkin, P. A. Nsumei, X. Huang, B. W. Reinisch, R. R. Anderson, M. K. Sleeper, and W. J. Hughes (2006), Distribution of density along magnetospheric field lines, *J. Geophys. Res.*, *111*, A04213, doi:10.1029/2005JA011414.
Drummond, W. E., and D. Pines (1962), Nonlinear stability of plasma oscillations, *Nucl. Fusion Suppl.*, *3*, 1049–1058.
Dysthe, K. B. (1971), Some studies of triggered whistler emissions, *J. Geophys. Res.*, *76*, 6915–6931, doi:10.1029/JA076i028p06915.
Fok, M.-C., R. B. Horne, N. P. Meredith, and S. A. Glauert (2008), Radiation belt environment model: Application to space weather nowcasting, *J. Geophys. Res.*, *113*, A03S08, doi:10.1029/2007JA012558.
Gendrin, R. (1961), Le guidage des whistlers par le champ magnetique, *Planet. Space Sci.*, *5*, 274, doi:10.1016/0032-0633(61)90096-4.
Ginzburg, V. L., and A. A. Rukhadze (1975), *Waves in Magnetoactive Plasma/2nd Revised Edition*, Moscow, Izdatel'stvo Nauka, Russian.
Glauert, S. A., and R. B. Horne (2005), Calculation of pitch angle and energy diffusion coefficients with the PADIE code, *J. Geophys. Res.*, *110*, A04206, doi:10.1029/2004JA010851.
Hashimoto, K., I. Kimura, and H. Kumagai (1977), Estimation of electron temperature by VLF waves propagating in directions near the resonance cone, *Planet. Space Sci.*, *25*, 871–877, doi:10.1016/0032-0633(77)90040-X.
Inan, U. S., and S. Tkalcevic (1982), Nonlinear equations of motion for Landau resonance interactions with a whistler mode wave, *J. Geophys. Res.*, *87*, 2363–2367, doi:10.1029/JA087iA04p02363.
Karpman, V. I., J. N. Istomin, and D. R. Shklyar (1974), Nonlinear theory of a quasi-monochromatic whistler mode packet in inhomogeneous plasma, *Plasma Phys.*, *16*, 685–703, doi:10.1088/0032-1028/16/8/001.
Karpman, V. I., I. N. Istomin, and D. R. Shkliar (1975), Effects of nonlinear interaction of monochromatic waves with resonant particles in the inhomogeneous plasma, *Phys. Scr.*, *11*, 278–284, doi:10.1088/0031-8949/11/5/008.
Katoh, Y., Y. Omura, and D. Summers (2008), Rapid energization of radiation belt electrons by nonlinear wave trapping, *Ann. Geophys.*, *26*, 3451–3456, doi:10.5194/angeo-26-3451-2008.
Kellogg, P. J., C. A. Cattell, K. Goetz, S. J. Monson, and L. B. Wilson III (2010), Electron trapping and charge transport by large amplitude whistlers, *Geophys. Res. Lett.*, *37*, L20106, doi:10.1029/2010GL044845.
Kellogg, P. J., C. A. Cattell, K. Goetz, S. J. Monson, and L. B. Wilson III (2011), Large amplitude whistlers in the magnetosphere observed with wind-waves, *J. Geophys. Res.*, *116*, A09224, doi:10.1029/2010JA015919.
Kennel, C. F., and H. E. Petschek (1966), Limit on stably trapped particle fluxes, *J. Geophys. Res.*, *71*, 1–28.
Kersten, K., et al. (2011), Observation of relativistic electron microbursts in conjunction with intense radiation belt whistler-mode waves, *Geophys. Res. Lett.*, *38*, L08107, doi:10.1029/2011GL046810.
Khrabrov, A. V., and B. U. Ö. Sonnerup (1998), Error estimates for minimum variance analysis, *J. Geophys. Res.*, *103*, 6641–6652.
Kolomenskii, A. A., and A. N. Lebedev (1963), Self-resonant particle motion in a plane electromagnetic wave, *Sov. Phys. Dokl.*, *7*, 745.
Laird, M. J., and F. B. Knox (1965), Exact solution for charged particle trajectories in an electromagnetic field, *Phys. Fluids*, *8*, 755–756, doi:10.1063/1.1761296.
Lauben, D. S., U. S. Inan, and T. F. Bell (2001), Precipitation of radiation belt electrons induced by obliquely propagating lightning-generated whistlers, *J. Geophys. Res.*, *106*, 29,745–29,770, doi:10.1029/1999JA000155.
Lauben, D. S., U. S. Inan, T. F. Bell, and D. A. Gurnett (2002), Source characteristics of ELF/VLF chorus, *J. Geophys. Res.*, *107*, 1429, doi:10.1029/2000JA003019.
Le Contel, O., et al. (2008), First results of the THEMIS search coil magnetometers, *Space Sci. Rev.*, *141*, 509–534, doi:10.1007/s11214-008-9371-y.
Li, W., J. Bortnik, R. M. Thorne, and V. Angelopoulos (2011a), Global distribution of wave amplitudes and wave normal angles of chorus waves using THEMIS wave observations, *J. Geophys. Res.*, *116*, A12205, doi:10.1029/2011JA017035.
Li, W., R. M. Thorne, J. Bortnik, Y. Y. Shprits, Y. Nishimura, V. Angelopoulos, C. Chaston, O. Le Contel, and J. W. Bonnell (2011b), Typical properties of rising and falling tone chorus waves, *Geophys. Res. Lett.*, *38*, L14103, doi:10.1029/2011GL047925.
Li, W., R. M. Thorne, J. Bortnik, X. Tao, and V. Angelopoulos (2012), Characteristics of hiss-like and discrete whistler-mode emissions, *Geophys. Res. Lett.*, *39*, L18106, doi:10.1029/2012GL053206.
Li, W., J. Bortnik, R. M. Thorne, C. M. Cully, L. Chen, V. Angelopoulos, Y. Nishimura, J. B. Tao, J. W. Bonnell, and O. LeContel (2013), Characteristics of the Poynting flux and wave normal vectors of whistler-mode waves observed on THEMIS, *J. Geophys. Res. Space Physics*, *118*, 1461–1471, doi:10.1002/jgra.50176.
Lyons, L. R. (1974), Pitch angle and energy diffusion coefficients from resonant interactions with ion-cyclotron and whistler waves, *J. Plasma Phys.*, *12*, 417–432, doi:10.1017/S002237780002537X.
Lyons, L. R., R. M. Thorne, and C. F. Kennel (1972), Pitch-angle diffusion of radiation belt electrons within the plasmasphere, *J. Geophys. Res.*, *77*, 3455–3474, doi:10.1029/JA077i019p03455.
Lyons, L. R., Y. Nishimura, X. Xing, A. Runov, V. Angelopoulos, E. Donovan, and T. Kikuchi (2012), Coupling of dipolarization front flow bursts to substorm expansion phase phenomena within the magnetosphere and ionosphere, *J. Geophys. Res.*, *117*, A02212, doi:10.1029/2011JA017265.
Means, J. D. (1972), Use of the three-dimensional covariance matrix in analyzing the polarization properties of plane waves, *J. Geophys. Res.*, *77*, 5551–5559, doi:10.1029/JA077i028p05551.
Millan, R. M., and D. N. Baker (2012), Acceleration of particles to high energies in Earth's radiation belts, *Space Sci. Rev.*, *173*, 103–131, doi:10.1007/s11214-012-9941-x.
Mourenas, D., A. Artemyev, O. Agapitov, and V. Krasnoselskikh (2012a), Acceleration of radiation belts electrons by oblique chorus waves, *J. Geophys. Res.*, *117*, A10212, doi:10.1029/2012JA018041.
Mourenas, D., A. V. Artemyev, J.-F. Ripoll, O. V. Agapitov, and V. V. Krasnoselskikh (2012b), Timescales for electron quasi-linear diffusion by parallel and oblique lower-band Chorus waves, *J. Geophys. Res.*, *117*, A06234, doi:10.1029/2012JA017717.
Nunn, D. (1971), Wave-particle interactions in electrostatic waves in an inhomogeneous medium, *J. Plasma Phys.*, *6*, 291, doi:10.1017/S0022377800006061.
Omura, Y., H. Matsumoto, D. Nunn, and M. J. Rycroft (1991), A review of observational, theoretical and numerical studies of VLF triggered emissions, *J. Atmos. Terr. Phys.*, *53*, 351–368.
Omura, Y., N. Furuya, and D. Summers (2007), Relativistic turning acceleration of resonant electrons by coherent whistler mode waves in a dipole magnetic field, *J. Geophys. Res.*, *112*, A06236, doi:10.1029/2006JA012243.
Panov, E. V., A. V. Artemyev, W. Baumjohann, R. Nakamura, and V. Angelopoulos (2013), Transient electron precipitation during oscillatory BBF braking: THEMIS observations and theoretical estimates, *J. Geophys. Res. Space Physics*, *118*, 3065–3076, doi:10.1002/jgra.50203.

Roberts, C. S., and S. J. Buchsbaum (1964), Motion of a charged particle in a constant magnetic field and a transverse electromagnetic wave propagating along the field, *Phys. Rev.*, *135*, 381–389, doi:10.1103/PhysRev.135.A381.
Romanov, Y. A., and G. F. Filippov (1961), The interaction of fast electron beams with longitudinal plasma waves, *Sov. Phys. JETP*, *13*, 87–92.
Roth, I., M. Temerin, and M. K. Hudson (1999), Resonant enhancement of relativistic electron fluxes during geomagnetically active periods, *Ann. Geophys.*, *17*, 631–638, doi:10.1007/s00585-999-0631-2.
Santolík, O., M. Parrot, and F. Lefeuvre (2003), Singular value decomposition methods for wave propagation analysis, *Radio Sci.*, *38*(1), 1010, doi:10.1029/2000RS002523.
Santolík, O., D. A. Gurnett, J. S. Pickett, M. Parrot, and N. Cornilleau-Wehrlin (2005), Central position of the source region of storm-time chorus, *Planet. Space Sci.*, *53*, 299–305, doi:10.1016/j.pss.2004.09.056.
Santolík, O., D. A. Gurnett, J. S. Pickett, J. Chum, and N. Cornilleau-Wehrlin (2009), Oblique propagation of whistler mode waves in the chorus source region, *J. Geophys. Res.*, *114*, A00F03, doi:10.1029/2009JA014586.
Sazhin, S. S., and M. Hayakawa (1992), Magnetospheric chorus emissions—A review, *Planet. Space Sci.*, *40*, 681–697, doi:10.1016/0032-0633(92)90009-D.
Shklyar, D., and H. Matsumoto (2009), Oblique whistler-mode waves in the inhomogeneous magnetospheric plasma: Resonant interactions with energetic charged particles, *Surv. Geophys.*, *30*, 55–104, doi:10.1007/s10712-009-9061-7.
Shklyar, D., J. Chum, and F. Jiřícek (2004), Characteristic properties of Nu whistlers as inferred from observations and numerical modelling, *Ann. Geophys.*, *22*, 3589–3606, doi:10.5194/angeo-22-3589-2004.
Shklyar, D. R. (1981), Stochastic motion of relativistic particles in the field of a monochromatic wave, *Sov. Phys. JETP*, *53*, 1197–1192.
Shklyar, D. R. (2011a), On the nature of particle energization via resonant wave-particle interaction in the inhomogeneous magnetospheric plasma, *Ann. Geophys.*, *29*, 1179–1188, doi:10.5194/angeo-29-1179-2011.
Shklyar, D. R. (2011b), Wave-particle interactions in marginally unstable plasma as a means of energy transfer between energetic particle populations, *Phys. Lett. A*, *375*, 1583–1587, doi:10.1016/j.physleta.2011.02.067.
Shprits, Y. Y., R. M. Thorne, R. B. Horne, and D. Summers (2006), Bounce-averaged diffusion coefficients for field-aligned chorus waves, *J. Geophys. Res.*, *111*, A10225, doi:10.1029/2006JA011725.
Shprits, Y. Y., D. A. Subbotin, N. P. Meredith, and S. R. Elkington (2008), Review of modeling of losses and sources of relativistic electrons in the outer radiation belt II: Local acceleration and loss, *J. Atmos. Sol. Terr. Phys.*, *70*, 1694–1713, doi:10.1016/j.jastp.2008.06.014.
Sibeck, D. G., and V. Angelopoulos (2008), THEMIS Science objectives and mission phases, *Space Sci. Rev.*, *141*, 35–59, doi:10.1007/s11214-008-9393-5.
Solovev, V. V., and D. R. Shkliar (1986), Particle heating by a low-amplitude wave in an inhomogeneous magnetoplasma, *Sov. Phys. JETP*, *63*, 272–277.
Subbotin, D., Y. Shprits, and B. Ni (2010), Three-dimensional VERB radiation belt simulations including mixed diffusion, *J. Geophys. Res.*, *115*, A03205, doi:10.1029/2009JA015070.
Summers, D., and B. Ni (2008), Effects of latitudinal distributions of particle density and wave power on cyclotron resonant diffusion rates of radiation belt electrons, *Earth Planets Space*, *60*, 763–771.
Summers, D., B. Ni, and N. P. Meredith (2007), Timescales for radiation belt electron acceleration and loss due to resonant wave-particle interactions: 1. Theory, *J. Geophys. Res.*, *112*, A04206, doi:10.1029/2006JA011801.
Tao, X., and J. Bortnik (2010), Nonlinear interactions between relativistic radiation belt electrons and oblique whistler mode waves, *Nonlinear Processes Geophys.*, *17*, 599–604, doi:10.5194/npg-17-599-2010.
Tao, X., J. Bortnik, R. M. Thorne, J. M. Albert, and W. Li (2012), Effects of amplitude modulation on nonlinear interactions between electrons and chorus waves, *Geophys. Res. Lett.*, *39*, L06102, doi:10.1029/2012GL051202.
Thorne, R. M., T. P. O'Brien, Y. Y. Shprits, D. Summers, and R. B. Horne (2005), Timescale for MeV electron microburst loss during geomagnetic storms, *J. Geophys. Res.*, *110*, A09202, doi:10.1029/2004JA010882.
Trakhtengerts, V. Y. (1966), Stationary states of the Earth's outer radiation zone, *Geomag. Aeron.*, *6*, 827–836.
Trakhtengerts, V. Y., M. J. Rycroft, D. Nunn, and A. G. Demekhov (2003), Cyclotron acceleration of radiation belt electrons by whistlers, *J. Geophys. Res.*, *108*, 1138, doi:10.1029/2002JA009559.
Tsurutani, B. T., B. J. Falkowski, O. P. Verkhoglyadova, J. S. Pickett, O. Santolík, and G. S. Lakhina (2011), Quasi-coherent chorus properties: 1. Implications for wave-particle interactions, *J. Geophys. Res.*, *116*, A09210, doi:10.1029/2010JA016237.
Ukhorskiy, A. Y., and M. I. Sitnov (2012), Dynamics of radiation belt particles, *Space Sci. Rev.*, *179*, 545–578, doi:10.1007/s11214-012-9938-5.
Varotsou, A., D. Boscher, S. Bourdarie, R. B. Horne, N. P. Meredith, S. A. Glauert, and R. H. Friedel (2008), Three-dimensional test simulations of the outer radiation belt electron dynamics including electron-chorus resonant interactions, *J. Geophys. Res.*, *113*, A12212, doi:10.1029/2007JA012862.
Vedenov, A. A., E. Velikhov, and R. Sagdeev (1962), Quasilinear theory of plasma oscillations, *Nucl. Fusion Suppl.*, *2*, 465–475.
Wilson III, L. B., C. A. Cattell, P. J. Kellogg, J. R. Wygant, K. Goetz, A. Breneman, and K. Kersten (2011), The properties of large amplitude whistler mode waves in the magnetosphere: Propagation and relationship with geomagnetic activity, *Geophys. Res. Lett.*, *38*, L17107, doi:10.1029/2011GL048671.
Zheng, Q., Y. Zheng, M.-C. Fok, and A. T. Y. Lui (2012), Electron energy diffusion and advection due to non-linear electron-chorus wave interactions, *J. Atmos. Sol. Terr. Phys.*, *80*, 152–160, doi:10.1016/j.jastp.2012.01.011.